Behavioral/Systems/Cognitive

During Fictive Locomotion, Graded Synaptic Currents Drive Bursts of Impulses in Swimmeret Motor Neurons

Brian Mulloney
Section of Neurobiology, Physiology, and Behavior, University of California, Davis, California 95616-8519

During forward swimming, motor neurons that innervate each crayfish swimmeret fire periodic coordinated bursts of impulses. These bursts occur simultaneously in neurons that are functional synergists but alternate with bursts in their antagonists. These impulses ride on periodic oscillations of membrane potential that occur simultaneously in neurons of each type. A model of the local circuit that generates this motor pattern has been proposed. In this model, each motor neuron is driven alternately by excitatory and inhibitory synaptic currents from nonspiking local interneurons. I tested this model by perturbing individual interneurons and recording synaptic currents and changes in input resistance from each class of motor neuron. I also simulated the synaptic currents that would be observed in a cell subject to different patterns of presynaptic input.

When the CNS was actively expressing the swimming motor pattern, changes in the membrane potential of individual local interneurons controlled firing of whole sets of motor neurons. Membrane currents in these motor neurons oscillated in phase with the motor output from their own local circuit. The phases of these oscillations differed in different functional classes of motor neurons. In neurons that could be clamped at the reversal potential of their outward currents, the model predicted that large periodic inward currents would be recorded. I observed no signs of periodic inward currents, even when the outward currents clearly had reversed.

These results permit a simplification of the cellular model. They are discussed in the context of neural control of locomotion in crustacea and insects.

Key words: **graded transmission; synaptic inhibition; coordination; locomotion; nonspiking local interneuron; bursting**

Introduction

When crayfish swim forward, the alternating power strokes and return strokes of their four pairs of swimmerets provide the necessary thrust. These periodic movements are driven by a centrally generated motor pattern (Hughes and Wiersma, 1960; Ikeda and Wiersma, 1964; Davis, 1968) that is expressed as the coordinated activity of ~600 motor neurons in four different abdominal ganglia, 75 motor neurons per swimmeret (Mulloney and Hall, 2000). These motor neurons fire bursts of action potentials at particular phases in each cycle of movements (see Fig. 1*A*). How do these bursts arise, and why are they so well coordinated?

The motor neurons that innervate one swimmeret are part of a module located in one-half of an abdominal ganglion. Each module includes four types of motor neurons (Mulloney and Hall, 1990, 2000): 35 power-stroke excitors (PSEs), 35 return-stroke excitors (RSEs), 2 power-stroke inhibitors (PSIs), and 3 return-stroke inhibitors (RSIs). Each module also includes a small set of nonspiking local interneurons, three intersegmental coordinating interneurons, and many sensory afferents from the swimmeret (Heitler and Pearson, 1980; Paul and Mulloney, 1985a,b; Killian and Page, 1992a,b; Namba and Mulloney, 1999). Bursts of spikes in each motor neuron ride on large oscillations of its membrane potential. If chemical synaptic transmission is blocked, these oscillations and impulses cease (Sherff and Mulloney, 1996).

The most effective synaptic input to motor neurons comes from the nonspiking local interneurons in each module. Skinner and Mulloney (1998) proposed that within each module three kinds of local nonspiking interneurons form a pattern-generating circuit. According to this model, these interneurons also drive the motor neurons with alternating excitatory and inhibitory synaptic currents (see Fig. 1*B*), and these currents are responsible for the coordinated firing of all the motor neurons. The model predicts, for example, that each member of the PSE pool receives periodic excitation simultaneously and that this excitation alternates with periodic inhibition. The model also predicts that the RSE pool receives periodic alternating excitation and inhibition, in antiphase with the inhibition and excitation of the PSEs.

In this paper, I demonstrate the control exerted by individual local interneurons on the activity of the swimmeret system. I also use discontinuous single-electrode voltage clamp (dSEVC) to examine the membrane currents that underlie oscillations of membrane potential in swimmeret motor neurons. During the phase of each cycle when the other members of their pool were silent, all neurons examined received periodic inhibitory synaptic currents. I found no evidence of periodic excitation in any of these neurons. At the point in the cycle when a neuron was firing, its

Received Feb. 19, 2003; revised April 15, 2003; accepted May 6, 2003.

This work was supported by National Science Foundation Grants IBN 97-28791 and 00-91284, and by Human Frontier Science Program Grant RG 61/98. I thank Wendy Hall for technical support.

Correspondence should be addressed to B. Mulloney, Section of Neurobiology, Physiology, and Behavior, University of California, Davis, One Shields Drive, Davis, CA 95616-8519. E-mail: bcmulloney@ucdavis.edu.

 0270-6474/03/235953-10$15.00/0

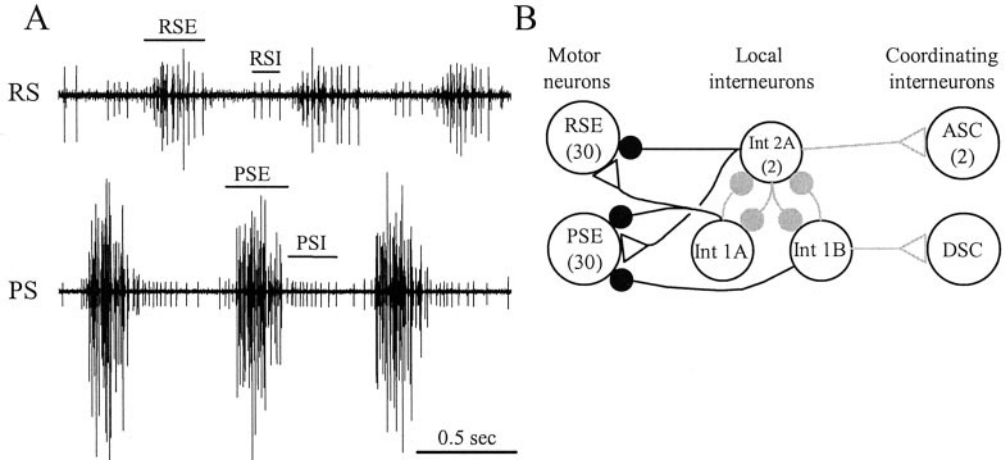

Figure 1. *A*, Extracellular recordings of impulses in the axons of swimmeret motor neurons recorded from the anterior branch (RS) and the posterior branch (PS) of the single nerve that innervates one swimmeret. This activity occurred spontaneously in an isolated ventral nerve cord, without pharmacological excitation. PSE, Power-stroke excitor; RSE, return-stroke excitor; PSI, power-stroke inhibitor; RSI, return-stroke inhibitor. *B*, A diagram of the Skinner and Mulloney (1998) model of the local circuit that drives alternating bursts in PS and RS motor neurons. Three types of nonspiking local interneurons (1A, 1B, 2A) make graded, monosynaptic connections with particular pools of motor neurons (PSE, RSE). Each motor neuron receives excitatory and inhibitory synapses that are active alternately because of the proposed reciprocal inhibition of the local interneurons. Three coordinating interneurons [ascending (ASC), descending (DSC)] are excited by the same local interneurons. The gray connections are not considered directly in this paper. Large open circles represent neurons; filled circles represent inhibitory synapses; open triangles represent excitatory synapses. Numbers in parentheses are the numbers of each type of neuron within each module.

input resistance was greater than it was when the neuron was silent. The results are not consistent with the assumptions of the model. In light of these results, I propose a simplification of our 1998 model that eliminates the periodic excitation of swimmeret motor neurons. These results also suggest that the synaptic organization of a swimmeret module is similar to that of the modules controlling walking legs in crustaceans and insects and that these results apply to locomotion in both phyla.

Materials and Methods

Crayfish, *Pacifastacus leniusculus* and *Procambarus clarkii*, were obtained from a commercial supplier (Crayfish International, Thornton CA) and maintained in aerated tanks of distilled water at a temperature between 12 and 15°C. Crayfish saline consisted of (in mM): 5.4 KCl, 2.6 $MgCl_2$, 13.5 $CaCl_2$, 195 NaCl, buffered with 10 mM Tris maleate at pH 7.4. Low Ca^{2+}–high Mg^{2+} saline consisted of (in mM): 5.4 KCl, 52 $MgCl_2$, 2.7 $CaCl_2$, 117 NaCl, buffered with 10 mM Tris maleate at pH 7.4. This low-Ca^{2+} saline reversibly suppressed chemical synaptic transmission (Sherff and Mulloney, 1996; Nakagawa and Mulloney, 2001). Our standard experimental solution contained either 1.5 or 3 μM carbachol in crayfish saline; 3 μM is approximately the ED_{50} of carbachol's excitation of the system (Mulloney, 1997). The preparation was superfused continually with aerated saline at a rate of 3 ml/min and maintained between 17° and 19°C.

Isolated ventral nerve cord preparation. Crayfish were first anesthetized on ice and then exsanguinated by replacing the hemolymph with crayfish saline. After exsanguination, the abdominal nervous system was removed from the animal and pinned out dorsal-side up on a Sylgard-lined dish. This preparation included ganglia A1 through A6. The dorsal sides of ganglia A2, A3, A4, and A5 were then desheathed with iridectomy scissors and forceps; ganglia A2 through A5 innervate swimmerets used for swimming.

Extracellular recording. The peripheral axons of the return-stroke (RS) and power-stroke (PS) motor neurons that innervate each swimmeret are segregated into anterior and posterior branches, respectively, of N1, the nerve that innervates the swimmeret (Mulloney and Hall, 2000). To record their impulses selectively (Fig. 1), I used pairs of pin electrodes on each branch of N1. Each pair of electrodes was connected through a switch-box to a stimulator and an amplifier so that it could be used either to stimulate or to record activity in the nerve. Signals from the pin electrodes were amplified, filtered, and recorded on VCR tape and on disk.

Intracellular recording. Glass microelectrodes were filled either with 2.5 M KAc + 0.1 M KCl + 5% Neurobiotin (Vector Labs, Burlingame CA) or with 1.0 M KAc + 0.05 M KCl + 1% 3 kDa Dextran-Texas Red (Molecular Probes, Eugene OR). These electrodes had resistances of ~35 MΩ. Signals from microelectrodes were buffered with an Axoclamp 2A or 2B amplifier (Axon Instruments, Union City CA), recorded on a VCR tape, and digitized with a Digidata 1200B board controlled by Clampex-8 (Axon Instruments).

Identification of swimmeret motor neurons. To record synaptic currents in these neurons, I used sharp microelectrodes to impale their processes in the lateral neuropil (LN), the anatomical locus of the pattern-generating circuit (Mulloney and Hall, 2000). To identify a motor neuron as a PSE, RSE, PSI, or RSI (Sherff and Mulloney, 1996, 1997), I recorded its impulses simultaneously from the microelectrode and from one of the peripheral branches of N1, the nerve that innervates the swimmeret. In an active preparation, PSE and RSI neurons fire bursts of impulses at about the same time (Fig. 1*A*), but their axons project out different branches so their impulses are recorded by different peripheral electrodes. RSE and PSI neurons can be distinguished by similar criteria. If antidromic stimulation of that branch then caused a short-latency, abrupt spike with a well defined threshold, the identification as a motor neuron was confirmed.

This paper reports the results of 24 experiments recorded from identified motor neurons and 11 experiments recorded from identified nonspiking local interneurons.

Identification of local interneurons. During an experiment, nonspiking local interneurons were identified tentatively by physiological criteria. These neurons showed no evidence of action potentials. When the preparation was expressing the swimmeret motor pattern, the potentials of these neurons oscillated in phase with the swimmeret system. Each interneuron reported here was filled with Neurobiotin (Vector Laboratories) or 3 kDa Dextran-Texas Red (Molecular Probes) during the experiment to confirm its identity using anatomical criteria (Paul and Mulloney, 1985a,b).

Discontinuous current clamp and single-electrode voltage clamp. To minimize the limiting effects of electrode capacitance on sampling rates during discontinuous current clamp (DCC) and dSEVC, I filled only the tip of the electrodes, coated the tip with Sylgard, used low-capacitance holders with a chlorided-silver wire in the shank, and kept the level of saline above the ganglion as low as possible. In DCC and dSEVC modes, the settling time of the microelectrode between each current pulse was

Table 1. Parameters in the simulation of synaptic currents

EL	−65 mV	E_{exc}	0 mV	E_{inh}	−80 mV
gL	0.3 mS/cm^2	g_{exc}	0.1 mS/cm^2	g_{inh}	0.1 mS/cm^2
V_{max}	10	V_{th}	−50	V_{slope}	10
τ_{S1}	10				

continually monitored on a dedicated oscilloscope. The sampling rate of the clamp circuit was adjusted to compensate for microelectrodes of different capacitance; 5 kHz was normally achieved. The clamp potential was controlled manually using the holding-position potentiometer of the clamp circuit. Currents were measured and recorded using the internal circuitry of the Axoclamp amplifier.

Two methods were used to isolate synaptically driven currents from the rest of the currents of a neuron. In experiments in which I recorded the membrane currents of a neuron both when the system was actively expressing the swimming motor pattern and then when the system was inactive, I subtracted the mean current recorded at each clamp potential during the inactive episode from the current recorded at that potential when the system was active. In experiments in which I recorded the currents of a neuron only when the system was active, I calculated the mean current recorded at each clamp potential and subtracted this mean current.

In two-microelectrode experiments, the clocks of the switching circuits in the two Axoclamps were synchronized. To reduce cross-talk between electrodes during DCC and dSEVC, I place a grounded aluminum blade between the microelectrodes, their holders, and the head-stages.

Fixation and visualization. At the end of each experiment, the preparation was transferred to another Sylgard-lined dish, pinned out again, and fixed with 4% paraformaldehyde overnight at 4°C. Tissues with Neurobiotin fills were then processed following the protocols described in Namba and Mulloney (1999), modified to visualize Neurobiotin with AlexaFluor-488 Streptavidin (Molecular Probes). All preparations were then cleared and examined as whole mounts under a confocal microscope to confirm the physiological identification of an interneuron with independent anatomical evidence.

Simulations of synaptic currents. The complete membrane current of the one-compartment model with two synapses is $I_{mem} = -I_{leak} - I_{exc} - I_{inh}$. Here the leakage current is $I_{leak} = gL \times (V - EL)$, the excitatory synaptic current is $I_{exc} = g_{exc} \times S1 \times (V - E_{exc})$, and the inhibitory current is $I_{inh} = g_{inh} \times S2 \times (V - E_{inh})$. In each of these equations, g is the conductance and E is the equilibrium potential for each current, and V is the clamped membrane potential. The value of each parameter is given in Table 1.

In the two synaptic equations, $S1$ and $S2$ control the extent to which each synaptic conductance is active. $S1$ and $S2$ are described by conventional first-order binding kinetics (Abbott and Marder, 1998): for $S1$, $dS1/dt = (S1\infty - S1)/((1 - S_1\infty) \times \tau S1)$ where $S1\infty = 0$ if $V_{pre1} \leq V_{th}$, otherwise $S1\infty = t_{anh}((V_{pre1} - V_{th})/V_{slope})$ and $V_{pre1} = V_{max} \times \sin(2\pi(t/per)) + V_{th}$. Here V_{max} is the potential at which release of transmitter by the synapse reaches its maximum, and V_{th} is the voltage threshold for release. The sine function allows the conductance to be active periodically in a graded manner. Similar equations control $S2$, except that $V_{pre2} = -V_{max} \times \sin(2\pi(t/per)) + V_{th}$, so that g_{exc} and g_{inh} are activated alternately. I used WinPP (Ermentrout, 2002) and Gear's method to integrate these equations.

Results

When the isolated ventral nerve cord was not actively expressing the swimming motor pattern, PSE motor axons were silent, while a few RSE and RSI axons fired steadily (Fig. 2). In these preparations, recordings from processes of most motor neurons within the LN showed that, except for irregular postsynaptic potentials (PSPs), their membrane potentials were steady.

When the system is active, membrane potentials of swimmeret motor neurons oscillate

If the preparation then began to express the motor pattern, PSE neurons fired bursts that became increasingly strong, and RSE and RSI neurons changed from steady firing to periodic bursting that alternated with these PSE bursts. Associated with these transitions, the membrane potentials of these neurons began to oscillate (Fig. 2). In this example, a bout of four cycles of activity is followed by an inactive interlude and finally by a transition to continuous expression of the swimming motor pattern. As the system became active, the membrane potential of an RSE motor neuron began to oscillate around its resting potential. During PSE bursts, this neuron was hyperpolarized, but it depolarized and fired impulses when PSE axons were silent.

Simultaneous recordings from PSE and RSE neurons showed that oscillations of their membrane potentials occurred in antiphase (Fig. 3), and these alternating depolarizations drove bursts of impulses in these motor neurons.

Individual nonspiking local interneurons can affect the whole population of motor neurons simultaneously

A small set of local, nonspiking interneurons with processes restricted to one LN are thought to be key components of the pattern-generating circuit in each swimmeret module (Heitler and Pearson, 1980; Paul and Mulloney, 1985a,b; Skinner and Mulloney, 1998). When the system is active, the membrane potentials of these interneurons also oscillate in phase with the motor output to each swimmeret (Fig. 4). Interneurons 1A and 1B (Int 1A, Int 1B) are depolarized during RS bursts, whereas interneurons 2A (Int 2A)are depolarized during PS bursts.

Experimental changes in the membrane potential of an individual nonspiking local interneuron affected the firing of many motor neurons in active preparations. In seven experiments, step depolarization of an Int 1A increased the numbers of spikes per burst in RSE neurons that were already firing and recruited additional RSE units (Fig. 4*Ai*). The same step inhibited PSE units and caused a PSI that had been firing bursts to fire continuously. In this figure, notice that the modulation of the membrane potential of Int 1A is reduced during the step but does not stop, and that the firing of PSI (on the PS trace) continued to be modulated. Notice too that it took three more cycles after the end of the step for the pattern to recover fully.

Hyperpolarization of this neuron also affected these different pools of motor neurons (Fig. 4*Aii*). RSE bursts were weakened and PSI firing ceased during the imposed hyperpolarization, but PSE increased and new PSE units were recruited.

The same manipulations of Int 2A had complementary effects on the output from the module (Fig. 4*B*). In four experiments, depolarization of an Int 2A inhibited RSE firing but increased the numbers of spikes per burst in PSE units (Fig. 4*Bi*). Hyperpolarization of Int 2A weakened the PSE bursts but elicited well structured RSE bursts (Fig. 4*Bii*). Neither PSI nor RSI units were active during this experiment.

These results are consistent with two features of our model: motor neurons receive excitation from one pair of these local interneurons but inhibition from the other (Fig. 1*B*). They do not prove that these features are correct.

Int 1A made a direct inhibitory connection with a PSE motor neuron

In an experiment with two microelectrodes in the same LN, I recorded PSPs in a PSE neuron that were driven by periodic pulses of current injected into the presynaptic 1A interneuron.

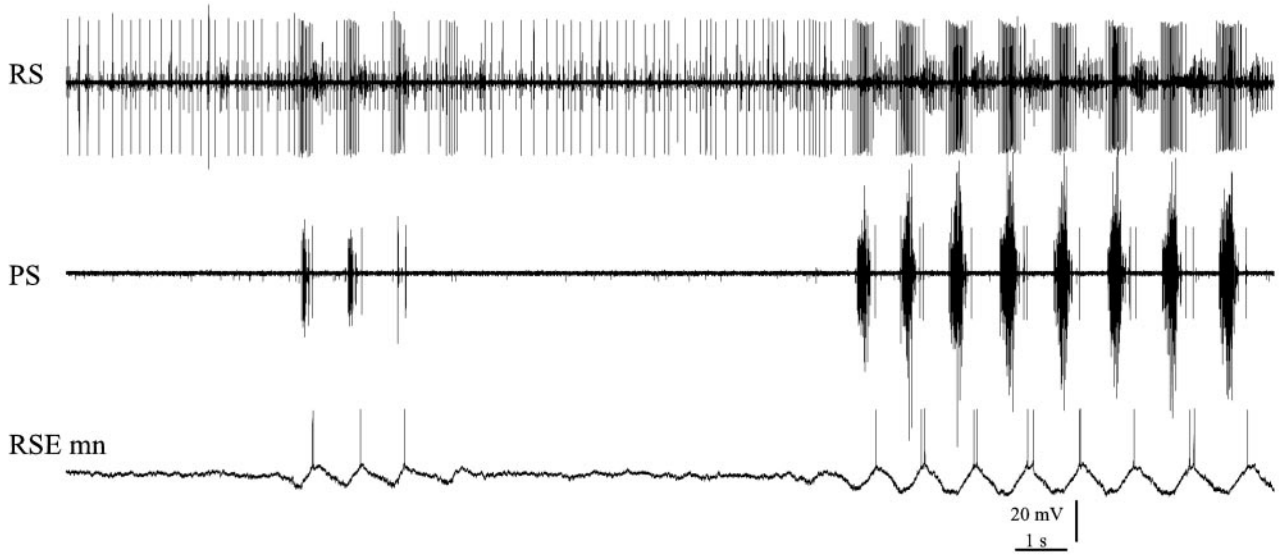

Figure 2. Two transitions from inactivity to expression of the swimming motor pattern. RSE mn, Intracellular recording from an RSE motor neuron; PS, extracellular recording from power-stroke branch of swimmeret nerve; RS, extracellular recording from return-stroke branch of swimmeret nerve. This recording was made from a *Procambarus clarkii* preparation. In this species, the RSI spikes recorded on RS during each PSE burst are characteristically larger than the spikes of their homologs in *Pacifastacus leniusculus* (Fig. 1*A*).

Each stimulus pulse was followed by an IPSP in the motor neuron (Fig. 5). The delay between the start of the stimulus pulse and the start of the IPSP was 2.2 msec, consistent with a monosynaptic connection (Nagayama and Sato, 1993; Nagayama et al., 1997). This synapse is explicitly part of the model.

Are bursts of firing in swimmeret motor neurons driven by alternating excitatory and inhibitory currents?

Using dSEVC and a microelectrode placed in its process in the LN (see Materials and Methods), it was possible to clamp the membrane potential of a motor neuron to a range of values around resting potential. Differences in the location of the electrode in separate experiments and inevitable limitations of space clamp caused some variation in quantitative features of the currents recorded in these experiments, but certain qualitative features emerged as characteristics of currents in different functional types of motor neurons.

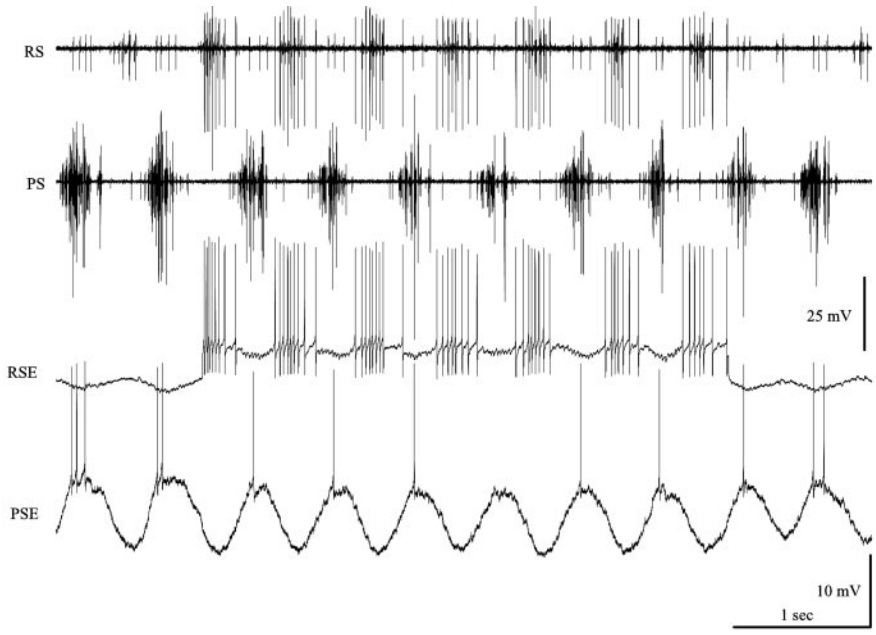

Figure 3. Simultaneous intracellular recordings from a power-stroke excitor (PSE) and a return-stroke excitor (RSE) motor neuron during expression of the swimmeret motor pattern. The membrane potentials of these antagonist neurons oscillated in antiphase, and bursts of impulses occurred whenever each neuron was depolarized. During part of this recording, the RSE neuron was depolarized by injecting a steady current to bring it above threshold. PS, RS, Extracellular recordings from power-stroke branch and return-stroke branch of swimmeret nerve.

If the preparation was not expressing the swimmeret motor pattern, the membrane currents of motor neurons clamped at rest potential were constant and showed no evidence of intrinsic oscillations (data not shown). If the preparation began actively to express the swimming motor pattern, the membrane currents of the same neurons alternated periodically, in phase with the firing of other neurons of the same functional type (Fig. 6). If the neuron was clamped at its nominal resting potential or at the midpoint of its voltage oscillations, its membrane currents alternated between inward and outward, in phase with the cycle of the module (Fig. 6). As expected, PSE neurons had inward currents during the PS bursts (Fig. 6*A*), and RSE neurons had inward currents during RS bursts (Fig. 6*B*). Some discrete PSCs were visible in these recordings; different neurons varied in this respect. Most of the current recorded in each neuron, however, appeared to be continuously varying and not composed of summed discrete PSCs from a few presynaptic sources.

Voltage clamping a motor neuron did not affect other neurons in the module and had no effect on the period or phase of the activity of the system (Fig. 6). Weak electrical coupling occurs between some synergist motor neurons, and polysynaptic inhibitory interactions occur between some antagonists (Heitler, 1978;

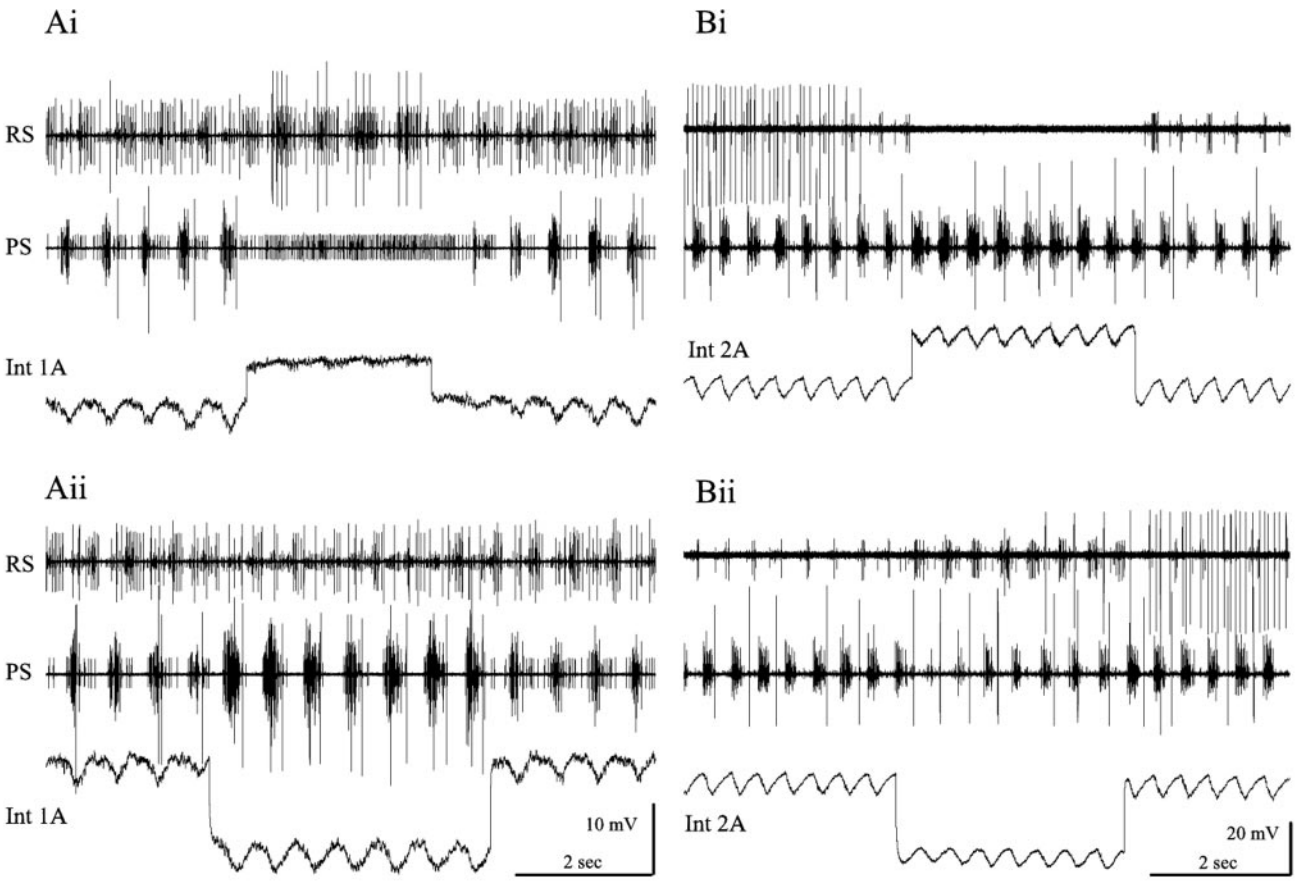

Figure 4. Oscillations of membrane potential in nonspiking local interneurons during expression of the swimming rhythm and the effects of these neurons on different types of motor neurons that innervate one swimmeret. *Ai*, *Aii*, The membrane potential of an interneuron 1A (Int 1A) was hyperpolarized whenever PSE bursts occurred. Experimental depolarization of this neuron inhibited all PSE firing, excited RSE firing, and allowed PSI to fire continuously. Experimental hyperpolarization inhibited PSI and weakened RSE bursts but increased the strength of each PSE burst. PS, RS, Extracellular recordings from power-stroke branch and return-stroke branch of swimmeret nerve. *Bi*, *Bii*, The membrane potential of a 2A interneuron (Int 2A) was depolarized whenever PSE bursts occurred. Experimental depolarization of this neuron elicited stronger PSE bursts but inhibited all RS activity. When the experimental depolarization stopped, RSE firing resumed. Experimental hyperpolarization excited RSE units but weakened PSE bursts. The large unit on the RS trace that was firing steadily at the start in *Bi* and resumes in *Bii* is not part of the swimmeret system. Its apparent correlation with stimulation of Int 2A is not reproducible.

Sherff and Mulloney, 1996). Currents injected into some motor neurons did affect the firing of some other neurons in the same module (Heitler, 1978; Sherff and Mulloney, 1996); the reduced number of spikes in the PSE neuron during depolarization of RSE recorded in Figure 3 is an example.

Synaptic currents in motor neurons during expression of the swimming motor pattern

Our 1998 model of the pattern-generating circuit within each module assumed that swimmeret motor neurons are driven by periodically alternating inhibitory and excitatory synaptic currents (Fig. 1*B*). If these currents result from periodic increases in membrane conductances caused by binding of transmitters to different ligand-gated channels, one selective for cations and another for chloride or potassium ions, then the inward currents should have a different reversal potential than the outward currents. In that case, clamping the membrane potential at the reversal potential of the outward currents should reveal periodic inward currents, larger than they had been when the neuron was clamped at resting potential.

Simulations

This notion was simulated mathematically by constructing a one-compartment passive cell that received two graded synaptic cur-

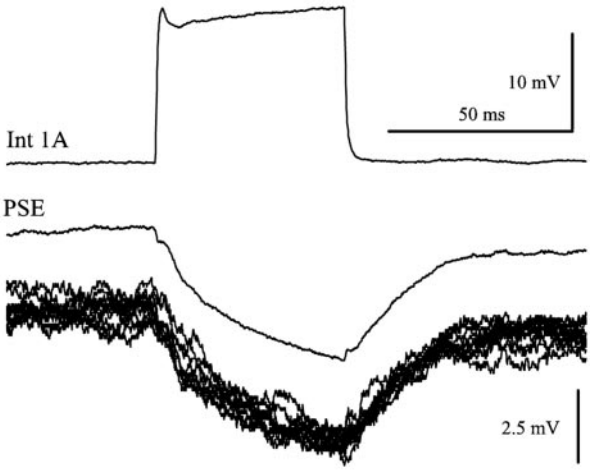

Figure 5. Int 1A made a monosynaptic connection with a PSE motor neuron. Int 1A was stimulated periodically with depolarizing pulses of current while the responses of the PSE motor neuron was recorded. This synapse had a delay of 2.2 msec. The pair of clean traces is the average of multiple sweeps, and the 10 raw PSE traces displaced below the average PSE response show the precision of these responses.

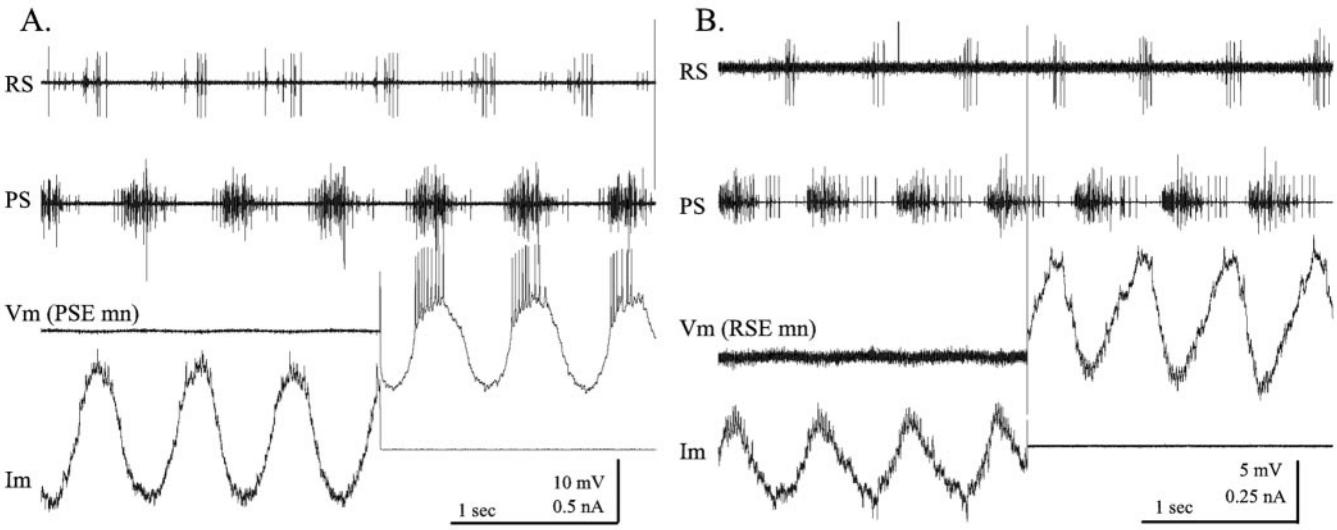

Figure 6. Membrane currents that underlie periodic depolarizations of motor neurons. In this and all subsequent recordings of membrane currents, inward currents are plotted as negative or downward. V_m, Membrane potential; I_m, membrane current. *A*, A PSE motor neuron, clamped below threshold during four cycles of activity and then released for three additional cycles. During dSEVC, V_m was −50 mV; during bridge mode, $I_m = 0$ nA. *B*, An RSE motor neuron, clamped for four cycles and then released. During dSEVC, clamp potential was −70 mV; during bridge mode, $I_m = 0$ nA. PS, RS, Extracellular recordings from power-stroke branch and return-stroke branch of swimmeret nerve.

rents. The gating of these currents was controlled by a sine function, and they were active alternately (see Materials and Methods). When the cell was clamped at different potentials, the membrane currents depended both on the clamp potential and on the phase of the sine function. The performance of this cell in response to an excitatory current, to an inhibitory current, and to alternating excitatory and inhibitory currents is shown in Figure 7. In each of these three cases, the cell was clamped at four potentials: −50, −65, −80, and −95 mV. Resting potential was −65 mV, and the reversal potential for the inhibitory current was −80 mV. In both cases in which there was an active excitatory current, this current grew as membrane potential increased and the inhibitory current reversed (Fig. 7).

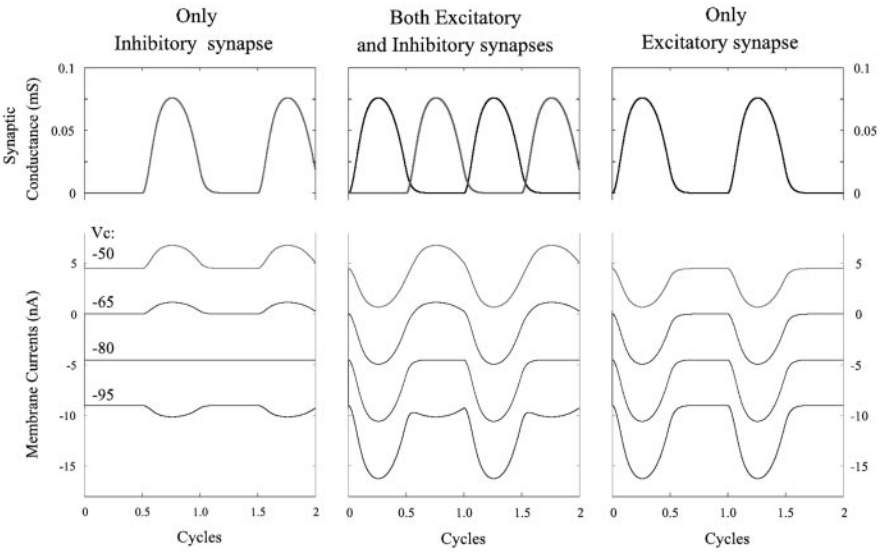

Figure 7. Simulations that show synaptic conductances and membrane currents in a one-compartment model subject to three patterns of periodic, graded synaptic input: only inhibition, alternating excitation and inhibition, and only excitation.

Experiments

I tested this prediction in 24 experiments; 6 of 13 PS neurons and 6 of 11 RS neurons were clamped well enough to demonstrate reversal of outward currents (Fig. 8). Because each neuron was clamped at each selected potential for many cycles of activity during these recordings, all of its transient voltage-gated currents were inactivated. The remaining periodic oscillations in membrane current observed whenever the system was actively expressing the swimming motor pattern I interpret as synaptically driven currents.

When a PSE neuron was clamped at a potential more depolarized than its resting potential (Fig. 8*A*, −51 mV), the magnitude of the oscillating membrane currents increased compared with those when it was clamped at resting potential. This was caused primarily by an increase in the inhibitory outward currents that occurred when the other PSE units were silent. In the example of Figure 8*A*, the discrete transient IPSCs that occurred during this phase were obviously larger when the neuron was clamped at −51 mV than they were when it was clamped at rest, −64 mV.

When the same neuron was clamped at a potential more hyperpolarized than resting potential, the magnitude of the current oscillations again increased. This increase was caused primarily by an increase in the inhibitory currents, now reversed by hyperpolarization to −83 mV. Notice the reversal of both the transient IPSCs and the graded IPSC that occurs between each PS burst.

Similar observations also apply to currents in RSE motor neurons (Fig. 8*B*). When an RSE neuron was clamped at a potential more depolarized than resting potential, the magnitude of the oscillations of its membrane currents increased (Fig. 8*B*, −55 mV), caused primarily by the growth of the periodic inhibitory outward current that occurred when PSE units were firing. When the neuron was clamped at a potential more hyperpolarized than rest (Fig. 8*B*, −85 mV), the inhibitory currents reversed.

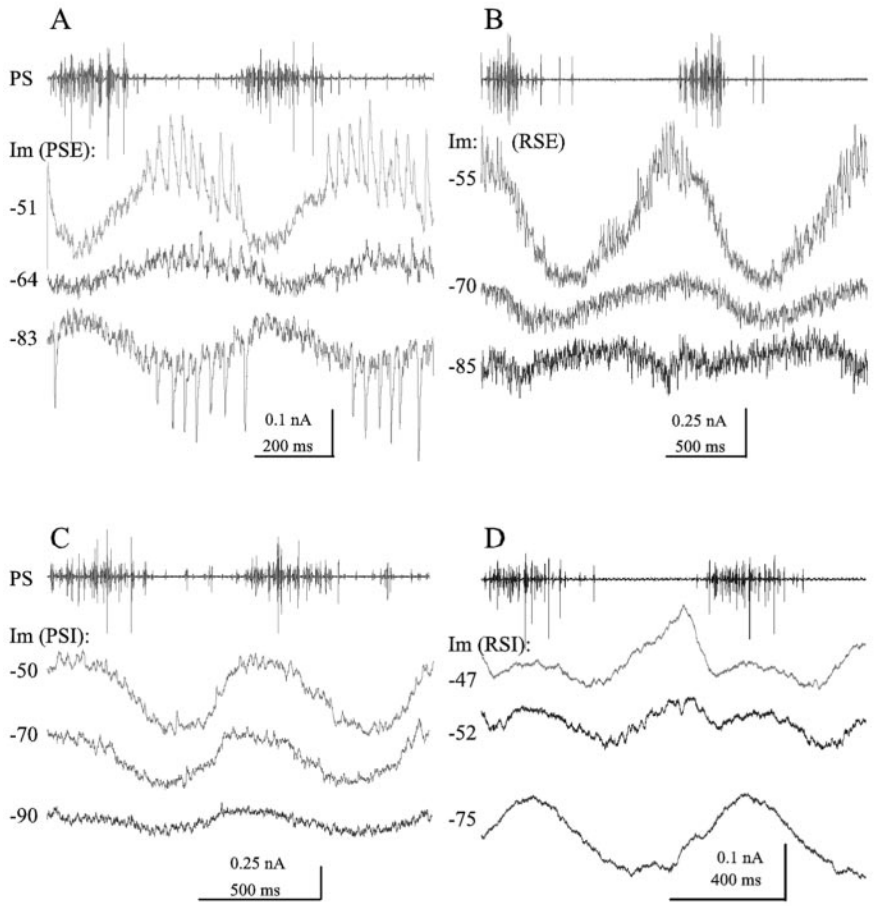

Figure 8. Synaptic currents in four types of swimmeret motor neurons during two complete cycles of the swimmeret motor pattern and power-stroke activity (PS) recorded simultaneously with one of the current recordings. *A*, Three recordings of membrane currents (I_m) from a PSE motor neuron during two cycles of the motor pattern. These voltage-clamp recordings were each triggered off the start of a PS burst (top trace) but made at different clamp potentials: −51, −64, and −83 mV. Raw recordings were low-pass filtered [cutoff frequency (fc), 500 Hz] but not averaged. Leakage currents recorded at the same clamp potentials when the system was silent were subtracted from the −64 and −83 mV traces; the mean current of the trace was subtracted from the −51 mV trace. Resting potential was −64 mV. Clamp parameters were as follows: sampling rate 5 kHz, gain 20, anti-alias filter 10. *B*, Three recordings of membrane currents from an RSE motor neuron made at different clamp potentials: −55, −70, and −85 mV. Each trace is the average of two or three raw traces that had been low-pass filtered (fc, 500 Hz), with leakage current corrected by subtracting the mean current of the averaged trace. Traces were aligned to the start of the first PS burst; the period of the −70 mV recording was longer than that of the other two, so the second cycle of the −70 mV current is somewhat delayed. Resting potential was −73 mV. Clamp parameters were as follows: sampling rate 5.7 kHz, gain >10, anti-alias filter 10. *C*, Three recordings of membrane currents from a PSI motor neuron, made at −50, −70, and −90 mV clamp potential. Resting potential was −53 mV. In this example, the outward inhibitory currents decreased with hyperpolarization but did not reverse. Each trace is a single sweep, low-pass filtered (fc, 500 Hz) but not averaged. Leakage current of each trace was corrected by subtracting the mean current. Clamp parameters were as follows: sampling rate 5 kHz, gain >50, anti-alias filter 5. *D*, Three recordings from an RSI motor neuron, made at −47, −52, and −75 mV clamp potential. Resting potential was −52 mV. Each trace is the average of between 7 and 10 single sweeps that were low-pass filtered (fc, 1 kHz). Leakage current of −75 trace was corrected by adding 0.5 nA. Clamp parameters were as follows: sampling rate 5.2 kHz, gain 25, anti-alias filter 20.

The currents recorded from PSI neurons (Fig. 8*C*) peaked at different phases than those in PSE neurons but flattened out as the clamp potential approached the reversal potential of the inhibitory current. In this example, probably because of the limitations of space clamp, I could not reverse the inhibitory current.

The currents recorded from RSI neurons (Fig. 8*D*) had the most complex periodic oscillations. When clamped at rest (Fig. 8*D*, −52 mV), they had two distinct outward "bumps" during each PS burst, followed by a brief interval of inward current, while PS units were silent. In this example, clamping the neuron to −75 mV reversed the first of these bumps but not the second.

If the assumption of a model was correct, I expected to see large inward currents alternating with the reversed outward currents plainly visible in these recordings (Fig. 7, middle panel). What is strikingly absent from these recordings is evidence of a periodic inward current that occurs in phase with the bursts of impulses in other neurons of the same type.

Input resistances of these neurons fluctuated periodically when the system was active

To examine the changes in conductance that caused these oscillations of membrane currents in active preparations, I used discontinuous current clamp to inject trains of 20 msec pulses of hyperpolarizing current into neurons. The period between pulses was >10 times the period of the motor pattern, and the timing of each pulse was independent of the phase of the motor pattern. The input resistance of the neuron was calculated from the size of each voltage transient and plotted as a function of the phase of the current pulse in the PS cycle of the module in which the neuron was located (Fig. 9).

The input resistance of each type of motor neuron that was tested oscillated measurably in phase with the motor pattern. The peak of resistance occurred at approximately the part of the cycle when the neuron was firing. PSE and RSI neurons peaked at approximately the same point in the cycle; PSI peaked later. The PSE neuron in this example was firing ~10 spikes per burst, so part of the increased scatter of points in the first half of the PSE plot in Figure 9 is probably attributable to the influence of its voltage-gated conductances.

Discussion

Whenever the system is actively expressing the motor pattern that drives coordinated swimmeret beating, the periodic bursts of impulses that occur in swimmeret motor neurons are driven by periodic currents that occur simultaneously in all neurons of the same functional type (Figs. 1, 6). We have proposed that these currents come from graded synapses onto all neurons in a pool (Skinner and Mulloney, 1998) and that it is this shared synaptic drive, rather than electrical coupling (Sherff and Mulloney, 1996), that produces simultaneous bursting in these neurons. Indirect evidence of this common synaptic drive comes from the orderly recruitment of units within each pool (Davis, 1971). In both the PSE and RSE pools, as excitation of the system increases, neurons with the smallest peripheral axons and therefore the smallest extracellularly recorded spikes are first to reach threshold (Figs. 2, 3, 4*Aii*).

Two observations documented in this paper led us to propose that each motor neuron receives alternating excitatory and inhib-

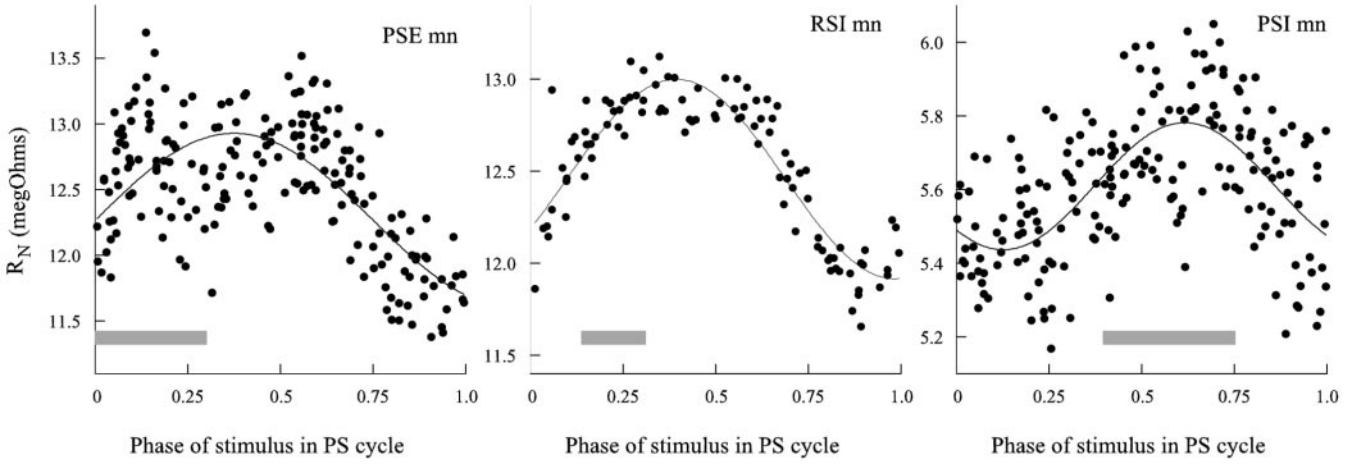

Figure 9. Periodic changes in the input resistance of swimmeret motor neurons during active expression of the swimming motor pattern. The gray boxes show when during the cycle each type of neuron was firing (compare Fig. 1*A*). Phase of stimulus was calculated as the phase in the cycle of PS bursting at which the current pulse began. The solid line in each plot is a best fit of the data to a periodic sine function

itory currents (Fig. 1*B*). First, when the system begins to express the swimming motor pattern, membrane potentials of motor neurons begin to oscillate. These oscillations often span the previously steady resting potential (Fig. 2). Alternating excitation and inhibition in the form of graded inward and outward currents would naturally drive periodic depolarization and hyperpolarization. Second, we knew that a small number of nonspiking local interneurons occur in each module (Paul and Mulloney, 1985a,b) and that these interneurons actively contribute to sculpting the motor pattern (Fig. 4). The effects of these neurons on antagonistic motor neurons are complementary (Fig. 4): if a local interneuron excites PSE, it inhibits RSE, and vice versa. One neuron that released the same transmitter at each of its synapses could have antagonistic effects on different target neurons if these targets expressed different receptors for that transmitter. If different local interneurons released different transmitters, then a neuron postsynaptic to two antagonist local interneurons could be excited by one interneuron and inhibited by the other if this postsynaptic neuron expressed the appropriate receptors selectively at different synapses.

In my new experiments, when a motor neuron was voltage clamped at its resting potential or at a potential in the middle of its oscillations (Figs. 6, 8, middle current traces), its membrane currents oscillated between inward and outward, in phase with the activity of the system. The simulations of a passive cell with alternating excitatory and inhibitory synapses, clamped at the reversal potential of the leak current (Fig. 7), illustrate that this behavior of the experimentally recorded currents is consistent with the two-synapse model. If these neurons were then clamped at potentials less polarized than rest, their outward currents grew (Fig. 8, top current traces), as theory and the two-synapse model would predict (Fig. 7). If these neurons were clamped at a potential near or greater than the inhibitory reversal potential, their outward currents disappeared or reversed as expected (Fig. 7, bottom current traces), but there was no evidence of periodic inward currents alternating with the reversed outward currents. Input resistances in these neurons dropped during that part of the cycle when the neuron was not firing (Fig. 9), as I would expect if an inhibitory conductance increase occurred then. This behavior is not consistent with the assumption of the model that these neurons receive periodic excitatory and inhibitory synaptic currents. Instead, it implies that in these preparations isolated from proprioceptive input, the only periodic currents that the pattern-generating neurons cause in motor neurons are inhibitory.

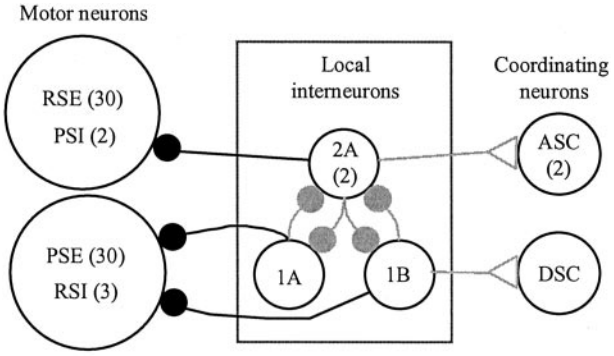

Figure 10. Diagram of the revised model of the local circuit in each swimmeret module that drives alternating bursts in swimmeret motor neurons. This diagram also incorporates symbols for the peripheral inhibitory motor neurons that in the past have been included only implicitly. Three types of nonspiking local interneurons (1A, 1B, 2A) make graded, monosynaptic inhibitory connections (black filled circles) with motor neurons of particular types (PSE, PSI, RSE, RSI). The numbers in parentheses are the numbers of neurons of each type in one module. The gray connections in this diagram were not examined in this paper. Large open circles represent neurons; filled circles represent inhibitory synapses; open triangles represent excitatory synapses.

These results permit a simplification of our 1998 model of the local pattern-generating circuit within each swimmeret module (Fig. 10). The key elements of this model continue to be the synaptic organization of four local interneurons: two Int 2A, one Int 1A, and one Int 1B (Skinner and Mulloney, 1998). The paired recordings in Figure 5 demonstrate that Int 1A did inhibit the PSE neuron directly, as the model assumed. In this revision, the different pools of motor neurons receive graded inhibitory synaptic input from particular local interneurons, but excitatory synapses have been stricken. The source of the inward currents in these neurons is not periodic.

These results also raise a problem: what causes swimmeret motor neurons to fire when the system is active? We know that when the system is inactive, motor neurons are not tonically inhibited because blocking synaptic transmission with low Ca^{2+}–high Mg^{2+} saline does not free them to fire continuously; instead, they are all silent (Sherff and Mulloney, 1996; Tschuluun

et al., 2001). Two classes of excitatory mechanisms might be present: tonic synaptic excitation by graded transmission from an unidentified premotor interneuron or modulation of currents intrinsic to the motor neurons. Experiments like those reported here use bath application of transmitter analogs to force stable expression of the motor pattern, but this tactic then confounds interpretation because the appearance of a tonic current in a neuron as the system becomes active might be the normal source of excitation, or it might be an independent response to the transmitter. One example is the response of different types of swimmeret motor neurons to crustacean cardioactive peptide, a peptide that also excites the swimmeret system: PSE and RSI neurons were directly excited by the peptide, but RSE and PSI were inhibited (Mulloney et al., 1997). Identification of a tonic excitatory current will require new experiments that measure membrane currents in preparations that express intermittent bouts of normal activity spontaneously, without applied drugs.

Another possible source of excitation must be modulation of intrinsic membrane currents in the motor neurons, either tonic currents or transient voltage-gated currents. A noninactivating Ca^{2+} current that activates above −60 mV occurs in swimmeret motor neurons (Chrachri, 1995), and a sustained, voltage-dependent outward current that is blocked by muscarinic agonists occurs in walking-leg motor neurons (Cattaert et al., 1994). Modulation of either of these currents could change the excitability of a neuron. A transient, voltage-gated inward current like I_h (Golowasch and Marder, 1992a) that was activated by hyperpolarization would produce a postinhibitory rebound (Perkel and Mulloney, 1974). Another candidate would be the voltage-dependent inward current that is the target of several modulatory pathways (Golowasch and Marder, 1992b; Swensen and Marder, 2000). The method I used in these experiments to record synaptic currents effectively inactivated all transient voltage-gated currents in the clamped neuron, so these data cannot identify any nonsynaptic currents that are normally at work in unclamped motor neurons.

The modules of swimmeret system are homologs of the neural circuits that control individual walking legs and scaphognathites in crustaceans (Mulloney et al., 2003), and the cores of the pattern-generating circuits controlling these other structures will probably prove to be the same as the kernel of the swimmeret modules (Fig. 10). Scaphognathite beating is regulated by nonspiking local interneurons (DiCaprio, 1989) and maintains a stable phase structure through a wide range of periods (DiCaprio et al., 1997). The motor patterns that drive the movements of walking legs are more complex than those that drive swimmeret movements, a complexity that reflects the larger number of joints in the leg. Both forward and backward walking have been recorded from isolated chains of thoracic ganglia (Chrachri and Clarac, 1990), and nonspiking local interneurons like those in the swimmeret system are premotor components of the walking system (Chrachri and Clarac, 1989). Like the swimmeret system (Braun and Mulloney, 1993; Chrachri and Neil, 1993), the walking system is also activated by muscarinic agonists (Chrachri and Clarac, 1987), and the anatomy of the thoracic ganglia is homologous to that of the abdominal ganglia (Mulloney et al., 2003).

The neural circuits that control walking legs of insects are also probably homologs of swimmeret modules. Each leg has its own set of motor neurons, controlled by its own set of nonspiking local interneurons (Burrows and Siegler, 1978, Burrows, 1980; Wolf and Laurent, 1994; Büschges, 1995; Wolf and Büschges, 1995). Pairs of these modules are located in each thoracic ganglion, one module in each half of the ganglion (Büschges et al., 1995). Each module can independently produce alternating bursts of impulses in antagonist motor neurons. The cholinergic pharmacology of these modules is very like that of crustacean walking and swimmeret systems; muscarinic analogs of acetylcholine elicit fictive locomotion from isolated thoracic ganglia (Ryckebusch and Laurent, 1993; Büschges et al., 1995). Like the synaptic currents in swimmeret motor neurons (Fig. 8), the synaptic currents recorded from insect leg motor neurons in isolated thoracic ganglia during fictive walking are exclusively inhibitory (Büschges, 1998). These currents arise from a decrease in input resistance and are carried by potassium ions (Büschges, 1998). However, when these leg modules have not been isolated experimentally, an additional synaptic component appears that comes from local proprioceptive feedback (Bässler and Büschges, 1998). When an isolated mesothoracic leg was stepping actively, these neurons were subject to two bouts of decreased input resistance in each cycle (Schmidt et al., 2001): one during the time the neuron was firing and one when it was inhibited. Comparable experiments on preparations with intact proprioceptive input have not yet been attempted in the swimmeret system.

References

Abbott LF, Marder E (1998) Modeling small networks. In: Methods in neuronal modeling (Koch C, Segev I, eds), pp 361–410. Cambridge, MA: MIT.

Bässler U, Büschges A (1998) Pattern generation for stick insect walking movements—multisensory control of a locomotor program. Brain Res Rev 27:65–88.

Braun G, Mulloney B (1993) Cholinergic modulation of the swimmeret system in crayfish. J Neurophysiol 70:2391–2398.

Burrows M (1980) The control of sets of motoneurones by local interneurons in the locust. J Physiol (Lond) 298:213–233.

Burrows M, Siegler MVS (1978) Graded synaptic transmission between local interneurons and motor neurons in the metathoracic ganglion of the locust. J Physiol (Lond) 285:231–256.

Büschges A (1995) Role of local nonspiking interneurons in the generation of rhythmic motor activity in the stick insect. J Neurobiol 27:488–512.

Büschges A (1998) Inhibitory synaptic drive patterns motoneuronal activity in rhythmic preparations of isolated thoracic ganglia in the stick insect. Brain Res 783:262–271.

Büschges A, Schmitz J, Bässler U (1995) Rhythmic patterns in the thoracic nerve cord of the stick insect induced by pilocarpine. J Exp Biol 198:435–456.

Cattaert D, Araque A, Buño W, Clarac F (1994) Nicotinic and muscarinic activation of motoneurons in the crayfish locomotor network. J Neurophysiol 72:1622–1633.

Chrachri A (1995) Ionic currents in identified swimmeret motor neurones of the crayfish *Pacifastacus leniusculus.* J Exp Biol 198:1483–1492.

Chrachri A, Clarac F (1987) Induction of rhythmic activity in motoneurons of crayfish thoracic ganglia by cholinergic agonists. Neurosci Lett 77:49–54.

Chrachri A, Clarac F (1989) Synaptic connections between motor neurons and interneurons in the fourth thoracic ganglion of the crayfish, *Procambarus clarkii.* J Neurophysiol 62:1237–1249.

Chrachri A, Clarac F (1990) Fictive locomotion in the fourth thoracic ganglion of the crayfish. J Neurosci 10:707–719.

Chrachri A, Neil DM (1993) Interaction and synchronization between two abdominal motor systems in crayfish. J Neurophysiol 69:1373–1383.

Davis WJ (1968) The neuromuscular basis of lobster swimmeret beating. J Exp Zool 168:363–378.

Davis WJ (1971) Functional significance of motoneuron size and soma position in swimmeret system of the lobster. J Neurophysiol 34:274–288.

DiCaprio RA (1989) Nonspiking interneurons in the ventilatory central pattern generator of the shore crab, *Carcinus maenas.* J Comp Neurol 285:83–106.

DiCaprio RA, Jordan G, Hampton T (1997) Maintenance of motor pattern phase relationships in the ventilatory system of the crab. J Exp Biol 20:963–974.

Ermentrout B (2002) Simulating, analyzing, and animating dynamical sys-

tems: a guide to XPPAUT for researchers and students. Philadelphia: SIAM.

Golowasch J, Marder E (1992a) Ionic currents of the lateral pyloric neuron of the stomatogastric ganglion of the crab. J Neurophysiol 67:318–331.

Golowasch J, Marder E (1992b) Proctolin activates an inward current whose voltage dependence is modified by extracellular Ca^{2+}. J Neurosci 12:810–817.

Heitler WJ (1978) Coupled motoneurones are part of the crayfish swimmeret central oscillator. Nature 275:231–234.

Heitler WJ, Pearson KG (1980) Non-spiking interactions and local interneurones in the central pattern generator of the crayfish swimmeret system. Brain Res 187:206–211.

Hughes GM, Wiersma CAG (1960) The coordination of swimmeret movements in the crayfish, *Procambarus clarkii.* J Exp Biol 37:657–670.

Ikeda K, Wiersma CAG (1964) Autogenic rhythmicity in the abdominal ganglion of the crayfish: the control of swimmeret movements. Comp Biochem Physiol 12:107–115.

Killian KA, Page CH (1992a) Mechanosensory afferents innervating the swimmerets of the lobster. I. Afferents activated by cuticular deformation. J Comp Physiol [A] 170:491–500.

Killian KA, Page CH (1992b) Mechanosensory afferents innervating the swimmerets of the lobster. II. Afferents activated by hair deflection. J Comp Physiol [A] 170:501–508.

Mulloney B (1997) A test of the excitability-gradient hypothesis in the swimmeret system of crayfish. J Neurosci 17:1860–1868.

Mulloney B, Hall WM (1990) GABAergic neurons in the crayfish nervous system: an immunocytochemical census of the segmental ganglia and stomatogastric system. J Comp Neurol 291:383–394.

Mulloney B, Hall WM (2000) Functional organization of crayfish abdominal ganglia. III. Swimmeret motor neurons. J Comp Neurol 419:233–243.

Mulloney B, Namba H, Agricola H-J, Hall WM (1997) Modulation of force during locomotion: differential action of crustacean cardioactive peptide on power-stroke and return-stroke motor neurons. J Neurosci 17:6872–6883.

Mulloney B, Tschuluun N, Hall WM (2003) Architechtonics of crayfish ganglia. Microsc Res Tech 60:253–265.

Nagayama T, Sato M (1993) The organization of exteroceptive information from the uropod to ascending interneurones of the crayfish. J Comp Physiol [A] 172:281–294.

Nagayama T, Aonuma H, Newland PL (1997) Convergent chemical and electrical synaptic inputs from proprioceptive afferents onto an identified intersegmental interneuron in the crayfish. J Neurophysiol 77:2826–2830.

Nakagawa H, Mulloney B (2001) A presynaptic basis for gradients in strength of synapses between different abdominal stretch-receptor axons and their common target neurons. J Neurosci 21:1645–1655.

Namba H, Mulloney B (1999) Coordination of limb movements: three types of intersegmental interneurons in the swimmeret system, and their responses to changes in excitation. J Neurophysiol 81:2437–2450.

Paul DH, Mulloney B (1985a) Nonspiking local interneuron in the motor pattern generator for the crayfish swimmeret. J Neurophysiol 54:28–39.

Paul DH, Mulloney B (1985b) Local interneurons in the swimmeret system of the crayfish. J Comp Physiol [A] 156:489–502.

Perkel DH, Mulloney B (1974) Motor pattern production in reciprocally inhibitory neurons exhibiting postinhibitory rebound. Science 185:181–183.

Ryckebusch S, Laurent G (1993) Rhythmic patterns evoked in locust leg motor neurons by the muscarinic agonist pilocarpine. J Neurophysiol 69:1583–1595.

Schmidt J, Fischer H, Büschges A (2001) Pattern generation for walking and searching movements of a stick insect leg. II. Control of motoneuronal activity. J Neurophysiol 85:354–361.

Sherff CM, Mulloney B (1996) Tests of the motor neuron model of the local pattern-generating circuits in the swimmeret system. J Neurosci 16:2839–2859.

Sherff CM, Mulloney B (1997) Passive properties of swimmeret motor neurons. J Neurophysiol 78:92–102.

Skinner FK, Mulloney B (1998) Intersegmental coordination of limb movements during locomotion: mathematical models predict circuits that drive swimmeret beating. J Neurosci 18:3831–3842.

Swensen AM, Marder E (2000) Multiple peptides converge to activate the same voltage-dependent current in a central pattern-generating circuit. J Neurosci 20:6752–6759.

Tschuluun N, Hall WM, Mulloney B (2001) Limb movements during locomotion: tests of a model of an intersegmental coordinating circuit. J Neurosci 21:7859–7869.

Wolf H, Laurent G (1994) Rhythmic modulation of the responsiveness of locust sensory local interneurons by walking pattern generating networks. J Neurophysiol 71:110–118.

Wolf H, Büschges A (1995) Nonspiking local interneurons in insect leg motor control. II. Role of nonspiking local interneurons in the control of leg swing during walking. J Neurophysiol 73:1861–1875.